Modeling and Performance Evaluation for Dual-Polarized Ricean MIMO Channels

Adrian Ispas*, Xitao Gong*, Christian Schneider†, Gerd Ascheid*, and Reiner Thomä†
*Chair for Integrated Signal Processing Systems, RWTH Aachen University, Germany
{ispas, gong, ascheid}@iss.rwth-aachen.de
†Institute of Information Technology, Ilmenau University of Technology, Germany
{christian.schneider, reiner.thomae}@tu-ilmenau.de

***Abstract*—Dual-polarized (DP) multiple-input multiple-output (MIMO) systems are known to be beneficial in terms of the spectral efficiency under certain conditions on the channel and the signal-to-noise ratio (SNR). In order to assess under which conditions DP antenna setups are advantageous over single-polarized (SP) antenna setups, an accurate yet analytically tractable modeling of such channels is a necessary but challenging task. We propose a novel channel model for DP mobile Ricean MIMO channels for which the statistical channel parameters are readily obtained from a moment-based channel decomposition. An approximate evaluation of the mutual information (MI), expressed as a function of the statistical channel parameters of the proposed channel model, is derived. This approximation allows to assess when it is beneficial in terms of the MI to switch from an SP to a DP setup. Finally, we evaluate the MI for selected SP and DP setups based on channel measurements at 2.53 GHz. We find that the DP setup only provides an improvement in terms of the MI in medium- to high-K-factor scenarios above a certain SNR. The approximate evaluation of the MI is able to accurately reproduce the SNR at which one should switch from an SP to the DP setup.**

I. Introduction

Multiple-input multiple-output (MIMO) transmission is by now a well established technique to enhance the spectral efficiency over wireless channels. While commonly antennas with the same polarization are considered for MIMO systems, the use of dual-polarized (DP) antennas is known to offer advantages in terms of the spectral efficiency under certain conditions on the channel and the signal-to-noise ratio (SNR). These conditions are not fully characterized and they can change over time, but it is known that DP MIMO systems are attractive in Ricean channels [1]. The spectral efficiency of single-polarized (SP) and DP MIMO systems has been compared in various contributions, see, e.g., [2]–[4]. Besides being able to improve the spectral efficiency, DP antennas allow for compact MIMO systems with co-located antennas due to the strong decorrelation over orthogonal polarizations. Considering that radio frequency chains are expensive components in a wireless system, one would like to keep their number low but still use the polarization domain of the channel when beneficial. A well-known solution is to perform antenna switching between differently polarized antennas.

In order to understand the channel properties under which different antenna setups maximize the spectral efficiency, one can resort to the use of channel models. The main goal of channel models is to give a simplified yet accurate representation of the effects of the channel on the received signal. They thus allow to replace the use of sophisticated channel measurements that are specific to a measurement environment, and, furthermore, they might allow for analytical evaluations. Several approaches to model the channel exist; they can be mainly classified in physical and analytical models [5]. A good overview on the modeling of DP MIMO channels can be found in [1], [2]. Unfortunately, an accurate and analytically tractable modeling of DP MIMO channels is a difficult task. One has to resort to several simplifying assumptions in order to obtain analytical expressions, e.g., for the mutual information (MI), and thus to be able to assess the influence of certain channel parameters on the spectral efficiency. Experimental results regarding DP MIMO channels are presented in, e.g., [1], [6], [7]. Furthermore, we mention contributions characterizing the orthogonality of DP MIMO channels [8] and the structure of Ricean channels regarding the diversity performance [9].

Contributions: We detail a general modeling approach for DP mobile Ricean MIMO channels. Furthermore, we evaluate the achievable rate over such channels when the transmitter (TX) has only statistical channel state information (CSI), while the receiver (RX) has instantaneous CSI. In particular, we contribute the following:

- We propose a general model as well as a moment-based channel decomposition for DP mobile Ricean MIMO channels yielding the statistical channel model parameters from measured data.
- We give an approximate evaluation of the achievable rate, i.e., the MI, which is an explicit function of the statistical parameters of the proposed channel model. We can thus assess the influence of the statistical channel parameters on the achievable rate.
- We evaluate the channel decomposition and the MI for selected 4×4 SP and DP MIMO setups based on urban macrocell measurements at 2.53 GHz. We find that the DP setup is only advantageous in terms of the MI for medium- to high-K-factor links above a certain SNR. The approximate evaluation of the MI reproduces the practically relevant crossing points between the MI of the SP and DP MIMO setups.

Notation: For a matrix $\mathbf{A}$, the (element-wise) complex conjugate, the transpose, and the conjugate transpose are

This work was supported by the Ultra high-speed Mobile Information and Communication (UMIC) research centre.

denoted by $\mathbf{A}^*$, $\mathbf{A}^T$, and $\mathbf{A}^H$, respectively. The trace and the rank of the matrix $\mathbf{A}$ are denoted by $\mathrm{tr}\{\mathbf{A}\}$ and $\mathrm{rank}\{\mathbf{A}\}$, respectively. For two matrices $\mathbf{A}$ and $\mathbf{B}$, $\mathbf{A} \odot \mathbf{B}$ is the Hadamard (element-wise) product and $\mathbf{A} \otimes \mathbf{B}$ is the Kronecker product. The vectorization, i.e., the column-wise stacking, of the matrix $\mathbf{A}$ is denoted by $\mathrm{vec}\{\mathbf{A}\}$. The $N \times N$ identity matrix is represented by $\mathbf{I}_N$. The $MN \times MN$ commutation matrix $\mathbf{K}_{M,N}$ fulfills $\mathbf{K}_{M,N}\,\mathrm{vec}\{\mathbf{A}\} = \mathrm{vec}\{\mathbf{A}^T\}$ for an $M \times N$ matrix $\mathbf{A}$. We use $[\mathbf{A}]_{k,l}$ to denote the element in the kth row and the lth column of $\mathbf{A}$, and we define $\mathbf{A}^+$ such that $[\mathbf{A}^+]_{k,l} = \max\{[\mathbf{A}]_{k,l}, 0\}$ holds. Expectation is denoted by $\mathrm{E}\{\cdot\}$, $\log(\cdot)$ is the logarithm to the base 2, and j is the imaginary unit.

II. System Model

We consider a MIMO channel characterized by time-varying and frequency-flat fading. The input-output relation for transmission from N_{TX} antennas at the TX to N_{RX} antennas at the RX is given at time slots $m \in \mathbb{Z}$ by the received signal

$$\mathbf{y}[m] = \mathbf{H}[m]\mathbf{x}[m] + \mathbf{n}[m] \tag{1}$$

where $\mathbf{y}[m]$ is a vector of length N_{RX}. The random channel matrices $\mathbf{H}[m]$ of size $N_{\mathrm{RX}} \times N_{\mathrm{TX}}$ are jointly proper. The zero-mean vectors $\mathbf{x}[m]$ of length N_{TX} denote the jointly proper Gaussian transmitted vectors that are uncorrelated in time with covariance matrix $\mathrm{E}\{\mathbf{x}[m]\mathbf{x}^H[m]\} = P_x\mathbf{Q}[m]$ and $\mathrm{tr}\{\mathbf{Q}[m]\} = 1$. The vectors $\mathbf{n}[m]$ of length N_{RX} are the white jointly proper Gaussian noise vectors in time with covariance matrix $\mathrm{E}\{\mathbf{n}[m]\mathbf{n}^H[m]\} = \sigma_n^2\mathbf{I}_{N_{\mathrm{RX}}}$. For ease of exposition, we define the (nominal) SNR $\rho = P_x/\sigma_n^2$. We assume the RX to have CSI, i.e., the RX has knowledge of the current channel realization $\mathbf{H}[m]$. The TX, on the other hand, only has statistical CSI of the channel.

III. Channel Modeling and Decomposition

A channel model has to be accurate yet simple enough to offer insight on the influence of the relevant channel parameters on the system performance. We choose the popular correlation-based analytical approach for MIMO channels [5] which is characterized by a multivariate proper Gaussian term representing the joint effects of a large number of independent scatterers. Additionally, a term representing line-of-sight (LOS) or a strong scatterer [10] can be added for each MIMO sub-link. The amplitude of the sub-links then changes from a Rayleigh to a Ricean distribution. The power distribution between these two terms is commonly represented by the K-factor, i.e., the ratio between the power of the dominant component and the power of the remaining weaker components.

A. Channel Model

Usually, the dominant components are represented by a deterministic rank-one matrix [11], [12]. This corresponds to, e.g., an LOS scenario where the TX and the RX are fixed. The situation is different when, e.g., a mobile terminal (MT) is present or channel realizations are picked at different frequencies. In this case, the dominant channel component has a varying phase and as a consequence the mean of the channel is zero [13]. We propose the following model for DP MIMO channels:

$$\mathbf{H}[m] = \underbrace{\begin{bmatrix} \bar{\mathbf{H}}_{\mathrm{VV}}[m] & \bar{\mathbf{H}}_{\mathrm{HV}}[m] \\ \bar{\mathbf{H}}_{\mathrm{VH}}[m] & \bar{\mathbf{H}}_{\mathrm{HH}}[m] \end{bmatrix}}_{=\bar{\mathbf{H}}[m]} + \underbrace{\begin{bmatrix} \tilde{\mathbf{H}}_{\mathrm{VV}}[m] & \tilde{\mathbf{H}}_{\mathrm{HV}}[m] \\ \tilde{\mathbf{H}}_{\mathrm{VH}}[m] & \tilde{\mathbf{H}}_{\mathrm{HH}}[m] \end{bmatrix}}_{=\tilde{\mathbf{H}}[m]} \tag{2}$$

with the $N_{\mathrm{TX},a} \times N_{\mathrm{RX},b}$ sub-matrices

$$\bar{\mathbf{H}}_{ab}[m] = \mathbf{V}_{ab}[m] \odot \mathbf{\Phi}_{ab}[m] \tag{3}$$

and $\tilde{\mathbf{H}}_{ab}[m]$ containing the sub-links with polarization a at the TX and b at the RX for $a, b \in \{\mathrm{V}, \mathrm{H}\}$. Here, V and H denote vertical and horizontal polarizations, respectively.[1] The number of vertical-polarized (VP) and the number of horizontal-polarized (HP) antennas at the TX are given by $N_{\mathrm{TX,V}}$ and $N_{\mathrm{TX,H}}$, respectively. We thus have $N_{\mathrm{TX,V}} + N_{\mathrm{TX,H}} = N_{\mathrm{TX}}$. The relations at the RX side are obtained analogously. In the SP case, we either use only VP or only HP antennas. In the DP case, we assume that, at both the TX and the RX, one half of the antennas is VP while the other half is HP. We split the dominant contributions into the deterministic amplitude matrix $\mathbf{V}_{ab}[m]$ and the random phase matrix $\mathbf{\Phi}_{ab}[m]$ with $[\mathbf{\Phi}_{ab}[m]]_{k,l} = e^{j\phi_{ab,(l-1)N_{\mathrm{RX}}+k}[m]}$ for $k = 1, \ldots, N_{\mathrm{RX},b}$ and $l = 1, \ldots, N_{\mathrm{TX},a}$. The remaining weaker scatterers are represented by the zero-mean proper Gaussian matrix $\tilde{\mathbf{H}}[m]$. As highlighted in [14], the challenging part is the modeling of the correlations between the phases of the dominant components in $\mathbf{\Phi}_{ab}[m]$. We first consider all MIMO sub-links with polarization a at the TX and b at the RX. For $p, q = 1, \ldots, N_{\mathrm{TX},a}N_{\mathrm{RX},b}$, we assume

1) $\phi_{ab,p}[m]$ is independent of $\tilde{\mathbf{H}}[m]$,
2) $\phi_{ab,p}[m]$ is uniformly distributed over $[-\pi, \pi)$,
3) $\Delta_{\phi,ab}^{p,q}[m] = \phi_{ab,p}[m] - \phi_{ab,q}[m]$ is deterministic.

The first two assumptions are commonly used. The last assumption follows from the assumption that all MIMO sub-links of the same polarization combination a and b observe the same dominant component and that the distance between the TX and the RX is considerably larger than the array sizes [15]. Clearly, for each polarization, we require the (directional) antennas at the TX and the RX to be oriented in the same direction.

Using assumption 3), we can rewrite (3) as

$$\bar{\mathbf{H}}_{ab}[m] = \mathbf{V}_{ab}[m] \odot \mathbf{\Delta}_{\phi,ab}[m]\; e^{j\phi_{ab}[m]},\; a, b \in \{\mathrm{V}, \mathrm{H}\} \tag{4}$$

where we defined $\phi_{ab}[m] = \phi_{ab,1}[m]$ and the deterministic matrix $\mathbf{\Delta}_{\phi,ab}[m] = \mathbf{\Phi}_{ab}[m]\; e^{-j\phi_{ab}[m]}$. In the following, we define the length $N_{\mathrm{TX}}N_{\mathrm{RX}}$ vectors $\mathbf{h}[m] = \mathrm{vec}\{\mathbf{H}[m]\}$, $\bar{\mathbf{h}}[m] = \mathrm{vec}\{\bar{\mathbf{H}}[m]\}$, and $\tilde{\mathbf{h}}[m] = \mathrm{vec}\{\tilde{\mathbf{H}}[m]\}$, and the $N_{\mathrm{TX}}N_{\mathrm{RX}} \times N_{\mathrm{TX}}N_{\mathrm{RX}}$ full correlation matrices of the channel

$$\mathbf{R}[m] = \mathrm{E}\{\mathbf{h}[m]\mathbf{h}^H[m]\} \tag{5}$$

$$\bar{\mathbf{R}}[m] = \mathrm{E}\{\bar{\mathbf{h}}[m]\bar{\mathbf{h}}^H[m]\} \tag{6}$$

$$\tilde{\mathbf{R}}[m] = \mathrm{E}\{\tilde{\mathbf{h}}[m]\tilde{\mathbf{h}}^H[m]\}. \tag{7}$$

[1] We note that other (orthogonal) polarization choices are possible as well; however, we choose vertical and horizontal polarizations as they often have different propagation characteristics, see [4] for an example in an indoor scenario.

Using assumption 1), it immediately follows that

$$\mathbf{R}[m] = \bar{\mathbf{R}}[m] + \tilde{\mathbf{R}}[m] \tag{8}$$

holds. We can categorize the MIMO sub-links into co-polarized links, i.e., links with VP to VP or HP to HP transmission, and into cross-polarized links, i.e., links with VP to HP or HP to VP transmission. Depending on whether the four polarizations combinations share a dominant component or not, the rank of $\bar{\mathbf{R}}[m]$ can vary. We show in Appendix A that generally we have $\operatorname{rank}\left\{\bar{\mathbf{R}}[m]\right\} \leq 4$. Now, consider the practically relevant setting that only the co-polarized links are affected by dominant components. Then, similarly as in Appendix A, it can be shown that $\operatorname{rank}\left\{\bar{\mathbf{R}}[m]\right\} \leq 2$ has to be fulfilled. Further specializing this setting to the case that vertical- and horizontal-polarized links are affected by two distinct dominant components with independent phase terms, it follows that $\bar{\mathbf{R}}[m]$ has rank two. When all polarization combinations share a common dominant component or when we consider an SP setup, the rank is one.

B. Channel Decomposition

We now describe a simple method to separate the contribution of the dominant channel components to the correlation matrix $\mathbf{R}[m]$ from the contributions of the remaining weaker scatterers. We note that in the mobile setting we cannot use the mean of the channel to decompose the channel into the dominant and the remaining channel components. We thus introduce a method to decompose the channel that is simple compared to high resolution parameter estimation techniques [16]. The method is inspired by the K-factor estimation in [17]. Compared to [15], we introduce a novel method that is suitable for both SP and DP MIMO channels.

We use the second- and fourth-order moments of the channel $\mathbf{R}[m] = \mathrm{E}\left\{\mathbf{h}[m]\mathbf{h}^H[m]\right\}$ and $\mathbf{T}[m] = \mathrm{E}\left\{(\mathbf{h}[m]\mathbf{h}^H[m])^2\right\}$, respectively, to obtain a simple solution to the channel decomposition of $\mathbf{R}[m] = \bar{\mathbf{R}}[m] + \tilde{\mathbf{R}}[m]$ into $\bar{\mathbf{R}}[m]$ and $\tilde{\mathbf{R}}[m]$. With the evaluation of $\mathbf{T}[m]$ in Appendix B, we immediately obtain the following relation:

$$\bar{\mathbf{R}}^2[m] = \mathbf{R}[m]\,\mathrm{tr}\left\{\mathbf{R}[m]\right\} + \mathbf{R}^2[m] - \mathbf{T}[m]. \tag{9}$$

With the eigendecomposition $\bar{\mathbf{R}}[m] = \bar{\mathbf{U}}[m]\bar{\mathbf{\Lambda}}[m]\bar{\mathbf{U}}^H[m]$, we have $\bar{\mathbf{R}}^2[m] = \bar{\mathbf{U}}[m]\bar{\mathbf{\Lambda}}^2[m]\bar{\mathbf{U}}^H[m]$ yielding the required eigenvectors and eigenvalues.

1) Dual-Polarized Channel: According to Section III-A, at most four eigenvalues of $\bar{\mathbf{R}}[m]$ are non-zero; however, only two are practically significant and smaller eigenvalues tend to be estimated less accurately. We thus have to exercise care in choosing the number of considered eigenvalues N_{DP}. In the following, we first find an estimate of $\bar{\mathbf{R}}[m]$ denoted as $\breve{\mathbf{R}}[m]$ according to (9). We then extract the N_{DP} largest eigenvalues of $\breve{\mathbf{R}}[m]$. Clearly, we have $N_{\mathrm{DP}} \leq 4$. The final estimate of $\bar{\mathbf{R}}[m]$ is

$$\bar{\mathbf{R}}^{(e)}[m] = \sum_{k=1}^{N_{\mathrm{DP}}} c_k[m]\breve{\mathbf{u}}_k[m]\breve{\mathbf{u}}_k^H[m] \tag{10}$$

where the vector $\breve{\mathbf{u}}_k[m]$ denotes the eigenvector corresponding to the kth largest eigenvalue $\breve{\lambda}_k[m]$ of $\breve{\mathbf{R}}[m]$. We now define the (positive semidefinite) estimates of $\mathbf{R}[m]$ and $\tilde{\mathbf{R}}[m]$ as $\mathbf{R}^{(e)}[m]$ and $\tilde{\mathbf{R}}^{(e)}[m]$, respectively. Moreover, we define $\breve{\mathbf{R}}_l[m] = \mathbf{R}^{(e)}[m] - \sum_{k=1}^{l} c_k[m]\breve{\mathbf{u}}_k[m]\breve{\mathbf{u}}_k^H[m]$ for $l = 0, \ldots, N_{\mathrm{DP}}$. The constants $c_k[m]$ for $k = 1, \ldots, N_{\mathrm{DP}}$ are chosen such that the positive semidefiniteness of $\tilde{\mathbf{R}}^{(e)}[m] = \mathbf{R}^{(e)}[m] - \bar{\mathbf{R}}^{(e)}[m]$ is ensured [18, Theorem 7.7.7]:

$$c_k[m] = \begin{cases} 0, \text{ for singular } \breve{\mathbf{R}}_{k-1}[m] \\ \min\left\{\breve{\lambda}_k^+[m], \left(\breve{\mathbf{u}}_k^H[m]\breve{\mathbf{R}}_{k-1}^{-1}[m]\breve{\mathbf{u}}_k[m]\right)^{-1}\right\}, \text{else.} \end{cases} \tag{11}$$

Note that some power of the dominant components corresponding to $\breve{\mathbf{u}}_k[m]$ is transferred to $\tilde{\mathbf{R}}^{(e)}[m]$ whenever $c_k[m] < \breve{\lambda}_k[m]$. This might occur when the estimates of the moments $\mathbf{R}[m]$ and $\mathbf{T}[m]$ are inaccurate.

2) Single-Polarized Channel: From Section III-A, we know that $\bar{\mathbf{R}}[m]$ must have rank one. We thus obtain the following estimate of $\bar{\mathbf{R}}[m]$:

$$\bar{\mathbf{R}}^{(e)}[m] = c_1[m]\breve{\mathbf{u}}_1[m]\breve{\mathbf{u}}_1^H[m]. \tag{12}$$

The constant $c_1[m]$ is chosen as in (11) to ensure the positive semidefiniteness of $\tilde{\mathbf{R}}^{(e)}[m]$.

IV. Performance Evaluation

With respect to the system model in Section II, the MI between the input $\mathbf{x}[m]$ and the output $\mathbf{y}[m]$ combined with CSI at the receiver is given in bit/channel use (bit/c.u.) by

$$\begin{aligned} &I\left(\mathbf{x}[m]; \mathbf{y}[m], \mathbf{H}[m]\right) \\ &= \mathrm{E}\left\{\log\det\left(\mathbf{I}_{N_{\mathrm{RX}}} + \rho\mathbf{H}[m]\mathbf{Q}[m]\mathbf{H}^H[m]\right)\right\}. \end{aligned} \tag{13}$$

We note that the time-dependent MI in (13) can be interpreted as an achievable rate for (non-stationary) slow- and fast-fading wireless channels [19], [20].

Based on a multivariate Taylor series expansion of $f(\mathbf{A}) = \log\det(\mathbf{A})$, we can state the following approximation of (13):

$$\begin{aligned} &I\left(\mathbf{x}[m]; \mathbf{y}[m], \mathbf{H}[m]\right) \\ &\approx I^{\text{approx}}\left(\rho, \mathbf{Q}[m], \mathbf{R}_{\mathrm{TX}}[m], \mathbf{Z}[m]\right) \\ &= \log\det\left(\mathbf{I}_{N_{\mathrm{TX}}} + \rho\mathbf{R}_{\mathrm{TX}}^*[m]\mathbf{Q}[m]\right) \\ &\quad - \frac{\log(e)\rho^2}{2}\mathrm{tr}\left\{\left(\mathbf{Q}^T[m] \otimes \mathbf{I}_{N_{\mathrm{TX}}}\right)\mathbf{Z}[m]\left(\mathbf{Q}[m] \otimes \mathbf{I}_{N_{\mathrm{TX}}}\right)\mathbf{W}[m]\right\} \end{aligned} \tag{14}$$

with the $N_{\mathrm{TX}} \times N_{\mathrm{TX}}$ matrix $\mathbf{R}_{\mathrm{TX}}[m] = \mathrm{E}\left\{\mathbf{H}^T[m]\mathbf{H}^*[m]\right\}$ and the $N_{\mathrm{TX}}^2 \times N_{\mathrm{TX}}^2$ matrices

$$\begin{aligned} \mathbf{W}[m] = \mathbf{K}_{N_{\mathrm{TX}}, N_{\mathrm{TX}}}\Big(&\left(\mathbf{I}_{N_{\mathrm{TX}}} + \rho\mathbf{R}_{\mathrm{TX}}^*[m]\mathbf{Q}[m]\right)^{-T} \\ &\otimes \left(\mathbf{I}_{N_{\mathrm{TX}}} + \rho\mathbf{R}_{\mathrm{TX}}^*[m]\mathbf{Q}[m]\right)^{-1}\Big) \end{aligned} \tag{15}$$

$$\begin{aligned} \mathbf{Z}[m] = \mathrm{E}\Big\{&\mathrm{vec}\left\{\mathbf{H}^H[m]\mathbf{H}[m] - \mathbf{R}_{\mathrm{TX}}^*[m]\right\} \\ &\times \left(\mathrm{vec}\left\{\mathbf{H}^H[m]\mathbf{H}[m] - \mathbf{R}_{\mathrm{TX}}^*[m]\right\}\right)^T\Big\}. \end{aligned} \tag{16}$$

The derivation is left out due to space constraints.

Additionally to $\mathbf{R}_{\mathrm{TX}}[m]$, (14) requires the evaluation of the fourth-order moment of the channel $\mathbf{Z}[m]$. In order to gain insight on the influence of typical channel parameters on the MI, we rewrite $\mathbf{Z}[m]$ as a function of $\bar{\mathbf{R}}[m]$ and $\tilde{\mathbf{R}}[m]$

only. Both of these parameters are available with the channel decomposition in Section III-B. Differently to [15], which only considered the SP case, we here restate (16) for SP and DP channels. To that end, we assume that only the co-polarized links are affected by dominant components. We then obtain

$$\mathbf{Z}[m] = \mathbf{K}_{N_{\text{TX}},N_{\text{TX}}}\tilde{\mathbf{Z}}[m] + \mathbf{K}_{N_{\text{TX}},N_{\text{TX}}}\breve{\mathbf{Z}}[m] + \breve{\mathbf{Z}}^T[m]\mathbf{K}_{N_{\text{TX}},N_{\text{TX}}} \tag{17}$$

with

$$\text{vec}\left\{\tilde{\mathbf{Z}}[m]\right\} = (\mathbf{I}_{N_{\text{TX}}} \otimes \mathbf{Y}[m])\,\text{vec}\left\{\tilde{\mathbf{R}}^*[m]\right\} \tag{18}$$

$$\text{vec}\left\{\breve{\mathbf{Z}}[m]\right\} = (\mathbf{I}_{N_{\text{TX}}} \otimes \mathbf{Y}[m])\,\text{vec}\left\{\bar{\mathbf{R}}^*[m]\right\} \tag{19}$$

and the $N_{\text{TX}}^3 \times N_{\text{TX}}N_{\text{RX}}^2$ block matrix $\mathbf{Y}[m]$ containing $\mathbf{I}_{N_{\text{TX}}} \otimes \tilde{\mathbf{U}}_{k,l}[m]$ in the kth row-partition and the lth column-partition for $k = 1, \ldots, N_{\text{TX}}$ and $l = 1, \ldots, N_{\text{RX}}$. The $N_{\text{TX}} \times N_{\text{RX}}$ matrix $\tilde{\mathbf{U}}_{k,l}[m]$ is defined by $\left[\tilde{\mathbf{U}}_{k,l}[m]\right]_{p,q} = \left[\tilde{\mathbf{R}}^*[m]\right]_{(k-1)N_{\text{RX}}+l,(p-1)N_{\text{RX}}+q}$ for $p = 1, \ldots, N_{\text{TX}}$ and $q = 1, \ldots, N_{\text{RX}}$. Due to space constraints, the derivation is left out.

V. Channel Measurements

We evaluate the previously obtained results using urban macrocell channel measurements that were performed at 2.53 GHz in 2 bands of 45 MHz in Ilmenau, Germany. During the measurement campaign the DP MIMO links from 3 base station (BS) positions with different heights to a multitude of MT tracks were measured sequentially. The MT was moving with a maximal velocity of about 10 km/h. In this paper, we extract the 20 MHz band centered at 2.505 GHz, and we use the 3 BS positions at a height of 25 m with the 3 MT reference tracks. For further details regarding the measurement campaign, see [21].

After a denoising step in the time-delay domain, we estimate the statistical quantities. To this end, the ensemble averaging is replaced by an averaging in time over $N_t = 16$ and in frequency over $N_f = 128$ samples. This yields a total of 2048 (≈ 500 non-coherent) realizations [21]. We normalize the channel matrices $\mathbf{H}[m]$ with a scalar factor such that $\text{E}\left\{||\mathbf{h}_{\text{co}}[m]||_F^2\right\} = N_{\text{co}}$ is fulfilled inside each stationarity region of size N_t in time and N_f in frequency. Here, $\mathbf{h}_{\text{co}}[m]$ is a vector containing only the elements of $\mathbf{H}[m]$ corresponding to co-polarized sub-links and N_{co} denotes their number. This guarantees a fair comparison between SP and DP setups since we account for the power loss in cross-polarized sub-links.

A. Antenna Setups

We choose a uniform linear array at the BS (TX) and two uniform circular arrays (UCAs), which lie on top of each other, at the MT (RX) for the subsequent evaluations. At the MT, we are thus able to differentiate between the following four orientations: the front (direction of motion), the back, and the two sides of the MT. We consider one DP antenna setup and two SP antenna setups, a VP and an HP setup, for the 4×4 MIMO case. We use co-located DP antennas at the TX and the RX separated by $3\lambda_c$ and $0.5\lambda_c$ (across the UCAs), respectively, for the DP setup. For the SP setups, the antennas are separated by λ_c at the TX and $0.5\lambda_c$ (different UCAs) or $0.327\lambda_c$ (same UCA) at the RX. Therefore, all setups result in the same array length at the TX.

TABLE I
Specification and Properties of the Reference Links

Link	BS	Track	MT orient.	MT pos. [m]	K-Factors
1	1	41a-42	back	$0 - 34.9$	low
2	3	9a-9b	left	$0 - 38.9$	medium
3	2	10b-9a	front	$9.8 - 56.8$	high
4	3	10b-9a	left	$0 - 64.9$	varying

TABLE II
Average K-factors from the measured channel and the proposed channel decomposition

	K-factors: Measurements				K-factors: Decomposition			
Link	**V-V**	**H-H**	**V-H**	**H-V**	**V-V**	**H-H**	**V-H**	**H-V**
1	0.5	0.8	0.4	0.4	0.5	0.6	0.3	0.3
2	1.6	1.4	0.6	0.7	1.2	0.9	0.2	0.2
3	4.0	5.7	1.9	1.8	4.0	5.4	1.7	1.5

B. Scenario Classification

Similar to [22], we arrange the measurements into links with low, medium, and high (co-polarized) K-factors, see Table I. The low K-factor links are characterized by K-factor values in $[0, 2]$, while the medium and high K-factors links have several peaks with values above 5 and 10, respectively. Additionally, we have one link with varying K-factors which consists of low and high K-factor parts. We observed that the cross-polarization discrimination and the correlation coefficients between co-polarized links increase with the K-factors. More details regarding the classification can be found in [15].

VI. Results

We first present results on the K-factors averaged over the sub-links of each polarization combination. In order to check the efficiency of the channel decomposition, we compare the K-factors from the decomposition to the ones obtained from the measurements with the moment method in [17]. In the following, we consider the practically relevant case of extracting $N_{\text{DP}} = 2$ eigenvalues, see Section III-B1. In Table II, we show the results for links 1-3 averaged over the driven distance. We see that the cross-polarized links, VP to HP (V-H) and HP to VP (H-V), show significantly smaller K-factors than the co-polarized ones, VP to VP (V-V) and HP to HP (H-H). In general, we observe lower K-factor values from the channel decomposition due to guaranteeing the positive semidefiniteness of the correlation matrices, see Section III-B. In Fig. 1, we depict the evolution over distance for link 4 as it is characterized by varying K-factors, see Table I. Similar obervations as in Table II can be made. Furthermore, we observe that the channel decomposition is able to reproduce the tendencies in the evolution of the measured K-factors.

We now compare the approximative evaluation of the MI, i.e., (14) with (15) and (17), using $N_{\text{DP}} = 2$, to the (exact) MI (13). We use the optimal input with respect to the Jensen bound on the MI, where the eigenvectors of $\mathbf{R}_{\text{TX}}^*[m]$ form the precoding and the power allocation is obtained by a simple water-filling strategy [23]. The results of links 1-3 are again accumulated over each track and shown as a function

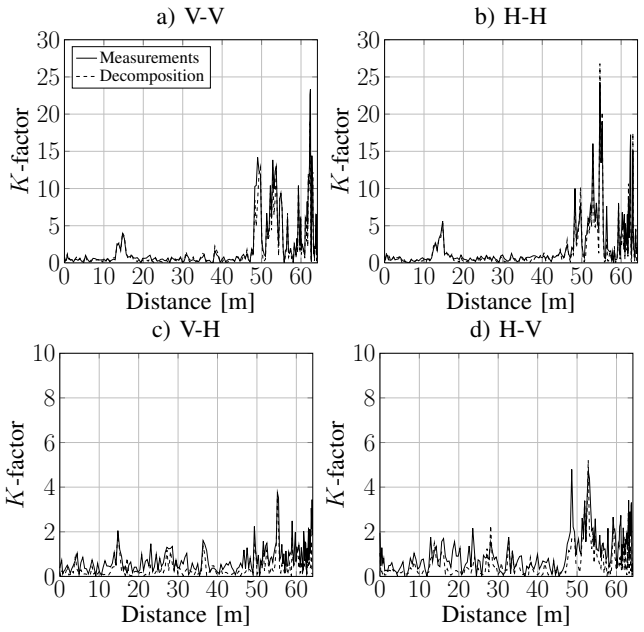

Fig. 1. K-factors vs. distance on link 4 (averaged over sub-links with the same polarization combination).

of the SNR in Fig. 2. The approximate evaluation of the MI is accurate; only at high SNRs a gap is noticeable. We see that the DP setup only provides an advantage in terms of the MI compared to the SP setups if the K-factors (of the co-polarized links) and the SNR attain certain values; the higher the K-factors, the lower this SNR threshold is. This is obvious as high K-factors significantly deteriorate the channel matrix conditioning in the SP case. Practically, a switching between SP and DP setups is thus most useful in medium- to high-K-factor scenarios; there the crossing points between the MI of the SP setups and the DP setup are accurately reproduced by the approximate evaluation of the MI. Furthermore, in Fig. 3, we plot the MI over distance for all three setups on link 4 at an SNR of 10 dB. We observe that the positions at which the DP setup outperforms the SP setups coincide with high K-factors, see Fig. 1.

VII. Conclusion

In this paper, we have studied the modeling of DP MIMO channels as well as the performance over such channels based on measurements at 2.53 GHz in an urban macrocell environment. We proposed a general channel model with a channel decomposition technique yielding the necessary statistical channel parameters. In order to gain some understanding on the statistical channel parameters influencing the MI, we derived an approximation of the MI which is a function of those parameters only. We found that our channel decomposition is able to separate a significant part of the contribution of the dominant channel components to the full correlation matrix. Moreover, we showed that the approximate evaluation of the MI is able to reproduce the crossing points between the MI of SP and DP setups. From the results, we conclude that the DP setup only provides a performance gain compared to the SP setups in medium- to high-K-factor channels above a certain SNR value.

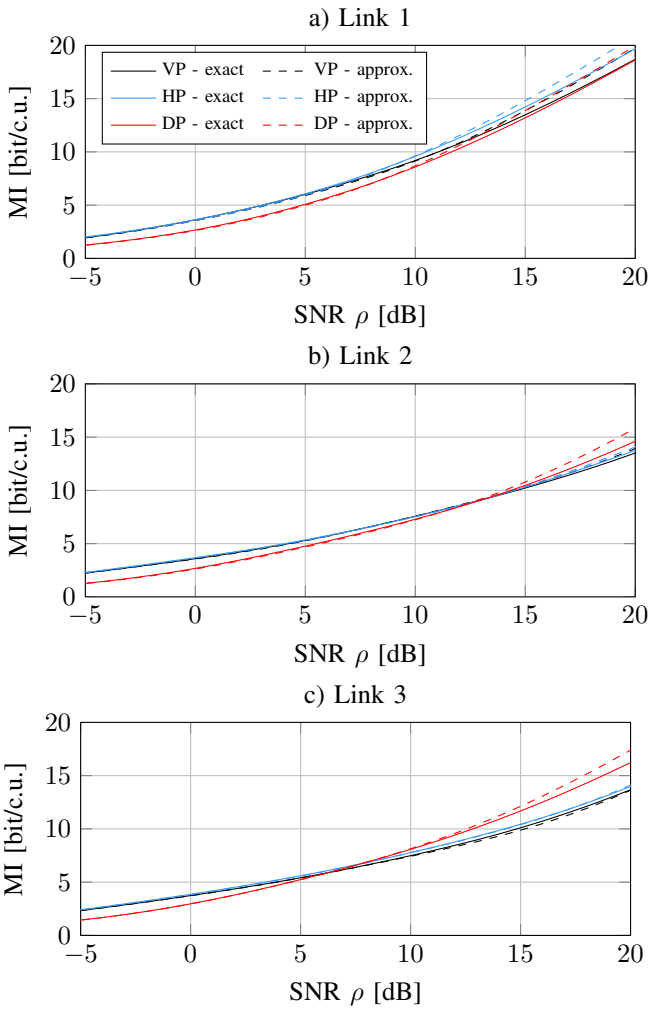

Fig. 2. MI vs. SNR of the exact and the approximate evaluation.

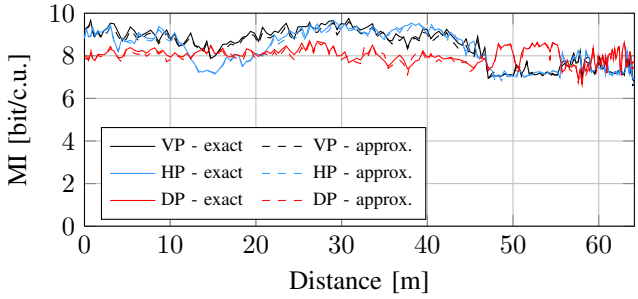

Fig. 3. MI vs. distance for the exact and the approximate evaluation on link 4 with an SNR $\rho = 10$ dB.

Appendix A
Rank of $\bar{\mathbf{R}}[m]$

We now drop the time argument to simplify the notation. In order to obtain a general condition on the rank of $\bar{\mathbf{R}}$, we first rearrange $\bar{\mathbf{R}}$ through column- and row-permutations with the permutation matrix $\mathbf{P}$ into $\bar{\mathbf{R}}_{\text{perm}} = \mathbf{P}\bar{\mathbf{R}}\mathbf{P}^T$ such that

$$\bar{\mathbf{R}}_{\text{perm}} = \begin{bmatrix} \bar{\mathbf{R}}_{\text{VVVV}} & \bar{\mathbf{R}}_{\text{VVVH}} & \bar{\mathbf{R}}_{\text{VVHV}} & \bar{\mathbf{R}}_{\text{VVHH}} \\ \bar{\mathbf{R}}_{\text{VHVV}} & \bar{\mathbf{R}}_{\text{VHVH}} & \bar{\mathbf{R}}_{\text{VHHV}} & \bar{\mathbf{R}}_{\text{VHHH}} \\ \bar{\mathbf{R}}_{\text{HVVV}} & \bar{\mathbf{R}}_{\text{HVVH}} & \bar{\mathbf{R}}_{\text{HVHV}} & \bar{\mathbf{R}}_{\text{HVHH}} \\ \bar{\mathbf{R}}_{\text{HHVV}} & \bar{\mathbf{R}}_{\text{HHVH}} & \bar{\mathbf{R}}_{\text{HHHV}} & \bar{\mathbf{R}}_{\text{HHHH}} \end{bmatrix} \tag{20}$$

with $\bar{\mathbf{R}}_{abcd} = \mathrm{E}\left\{\mathrm{vec}\left\{\bar{\mathbf{H}}_{ab}\right\}\left(\mathrm{vec}\left\{\bar{\mathbf{H}}_{cd}\right\}\right)^H\right\}$ for $a,b,c,d \in \{\mathrm{V},\mathrm{H}\}$ holds. It can be shown that

$$\bar{\mathbf{R}}_{\text{perm}} = \left(\mathbf{v}\mathbf{v}^H\right) \odot \left(\mathbf{d}_\phi \mathbf{d}_\phi^H\right) \odot \left(\mathbf{G} \otimes \mathbf{1}_{\frac{N_{\text{TX}}N_{\text{RX}}}{4}}\right) \quad (21)$$

where $\mathbf{v}$ and $\mathbf{d}_\phi$ are vectors containing amplitude and phase difference terms, respectively, holds. We further have

$$\mathbf{G} = \begin{bmatrix} 1 & g_{\text{VVVH}} & g_{\text{VVHV}} & g_{\text{VVHH}} \\ g_{\text{VHVV}} & 1 & g_{\text{VHHV}} & g_{\text{VHHH}} \\ g_{\text{HVVV}} & g_{\text{HVVH}} & 1 & g_{\text{HVHH}} \\ g_{\text{HHVV}} & g_{\text{HHVH}} & g_{\text{HHHV}} & 1 \end{bmatrix} \quad (22)$$

with $g_{abcd} = \mathrm{E}\left\{e^{j(\phi_{ab}-\phi_{cd})}\right\}$ for $a,b,c,d \in \{\mathrm{V},\mathrm{H}\}$ and the all-one matrix $\mathbf{1}_N$ of size $N \times N$. As the rank of a matrix is unchanged by left or right multiplication with a non-singular matrix [18, Section 0.4.6 (b)], it is obvious that $\mathrm{rank}\left\{\bar{\mathbf{R}}\right\} = \mathrm{rank}\left\{\bar{\mathbf{R}}_{\text{perm}}\right\}$ holds. Using $\mathrm{rank}\left\{\mathbf{A}\odot\mathbf{B}\right\} \leq \mathrm{rank}\left\{\mathbf{A}\right\}\mathrm{rank}\left\{\mathbf{B}\right\}$ [24, Theorem 5.1.7] and $\mathrm{rank}\left\{\mathbf{G}\right\} \leq 4$ with (21), we immediately obtain the inequality

$$\mathrm{rank}\left\{\bar{\mathbf{R}}\right\} \leq 4. \quad (23)$$

Appendix B
Evaluation of the Fourth-Order Moment $\mathbf{T}[m]$

We now evaluate the fourth-order moment $\mathbf{T}[m]$, where we drop the time argument for notational simplicity:

$$\begin{aligned}
\mathbf{T} &= \mathrm{E}\left\{\mathbf{h}\mathbf{h}^H\mathbf{h}\mathbf{h}^H\right\} \\
&\overset{(a)}{=} \mathrm{E}\left\{\bar{\mathbf{h}}\bar{\mathbf{h}}^H\bar{\mathbf{h}}\bar{\mathbf{h}}^H\right\} + \mathrm{E}\left\{\tilde{\mathbf{h}}\tilde{\mathbf{h}}^H\tilde{\mathbf{h}}\tilde{\mathbf{h}}^H\right\} + \bar{\mathbf{R}}\tilde{\mathbf{R}} + \tilde{\mathbf{R}}\bar{\mathbf{R}} \\
&\quad + \mathrm{E}\left\{\bar{\mathbf{h}}\,\mathrm{tr}\left\{\tilde{\mathbf{R}}\right\}\bar{\mathbf{h}}^H\right\} + \mathrm{E}\left\{\tilde{\mathbf{h}}\,\mathrm{tr}\left\{\bar{\mathbf{R}}\right\}\tilde{\mathbf{h}}^H\right\} \\
&\overset{(b)}{=} \bar{\mathbf{R}}\,\mathrm{tr}\left\{\bar{\mathbf{R}}\right\} + \tilde{\mathbf{R}}^2 + \tilde{\mathbf{R}}\,\mathrm{tr}\left\{\tilde{\mathbf{R}}\right\} + \bar{\mathbf{R}}\tilde{\mathbf{R}} \\
&\quad + \tilde{\mathbf{R}}\bar{\mathbf{R}} + \bar{\mathbf{R}}\,\mathrm{tr}\left\{\tilde{\mathbf{R}}\right\} + \tilde{\mathbf{R}}\,\mathrm{tr}\left\{\bar{\mathbf{R}}\right\} \\
&\overset{(c)}{=} \mathbf{R}\,\mathrm{tr}\left\{\mathbf{R}\right\} + \mathbf{R}^2 - \bar{\mathbf{R}}^2. \quad (24)
\end{aligned}$$

In (a), we used $\mathrm{E}\left\{\tilde{\mathbf{h}}\right\} = \mathbf{0}_{N_{\text{TX}}N_{\text{RX}},1}$, $\mathrm{E}\left\{\tilde{\mathbf{h}}\right\} = \mathbf{0}_{N_{\text{TX}}N_{\text{RX}},1}$, the mutual independency of $\bar{\mathbf{h}}$ and $\tilde{\mathbf{h}}$, and that $\mathrm{E}\left\{\tilde{\mathbf{h}}\tilde{\mathbf{h}}^T\right\} = \mathbf{0}_{N_{\text{TX}}N_{\text{RX}},N_{\text{TX}}N_{\text{RX}}}$ holds due to properness of $\tilde{\mathbf{h}}$. Here, $\mathbf{0}_{N_1,N_2}$ denotes the all-zero matrix of size $N_1 \times N_2$. In (b), we made use of the fact that $\bar{\mathbf{h}}^H\bar{\mathbf{h}} = \mathrm{tr}\left\{\bar{\mathbf{R}}\right\}$, and we used [25, Theorem 1] for the second term on the right hand side of (a). In (c), we used $\mathbf{R} = \bar{\mathbf{R}} + \tilde{\mathbf{R}}$.

References

[1] C. Oestges, B. Clerckx, M. Guillaud, and M. Debbah, "Dual-polarized wireless communications: From propagation models to system performance evaluation," *IEEE Trans. Wireless Commun.*, vol. 7, no. 10, pp. 4019–4031, Oct. 2008.

[2] M. Coldrey, "Modeling and capacity of polarized MIMO channels," in *Proc. 67th IEEE Veh. Technol. Conf. (VTC)*, Singapore, May 2008, pp. 440–444.

[3] V. R. Anreddy and M. A. Ingram, "Capacity of measured Ricean and Rayleigh indoor MIMO channels at 2.4 GHz with polarization and spatial diversity," in *Proc. IEEE Conf. Wireless Commun. and Netw. (WCNC)*, Las Vegas, NV, USA, Apr. 2006, pp. 946–951.

[4] P. Kyritsi, D. C. Cox, R. A. Valenzuela, and P. W. Wolniansky, "Effect of antenna polarization on the capacity of a multiple element system in an indoor environment," *IEEE J. Sel. Areas Commun.*, vol. 20, no. 6, pp. 1227–1239, Aug. 2002.

[5] P. Almers *et al.*, "Survey of channel and radio propagation models for wireless MIMO systems," *EURASIP J. Wireless Commun. Netw.*, vol. 2007, no. 1, Jan. 2007.

[6] V. Degli-Esposti, V.-M. Kolmonen, E. M. Vitucci, and P. Vainikainen, "Analysis and modeling on co- and cross-polarized urban radio propagation for dual-polarized MIMO wireless systems," *IEEE Trans. Antennas Propag.*, vol. 59, no. 11, pp. 4247–4256, Nov. 2011.

[7] F. Quitin, C. Oestges, F. Horlin, and P. De Doncker, "Polarization measurements and modeling in indoor NLOS environments," *IEEE Trans. Wireless Commun.*, vol. 9, no. 1, pp. 21–25, Jan. 2010.

[8] R. Tian, B. K. Lau, and J. Medbo, "Impact of Rician fading on the orthogonality of dual-polarized macrocellular channels," in *Proc. 6th European Conf. Antennas and Propag. (EUCAP)*, Prague, Czech Republic, Mar. 2012, pp. 447–451.

[9] R. Nabar, H. Bölcskei, and A. Paulraj, "Diversity and outage performance in space-time block coded Ricean MIMO channels," *IEEE Trans. Wireless Commun.*, vol. 4, no. 5, pp. 2519–2532, Sep. 2005.

[10] S. Wyne, A. F. Molisch, P. Almers, G. Eriksson, J. Karedal, and F. Tufvesson, "Outdoor-to-indoor office MIMO measurements and analysis at 5.2 GHz," *IEEE Trans. Veh. Technol.*, vol. 57, no. 3, pp. 1374–1386, May 2008.

[11] S. Jin, X. Gao, and X. You, "On the ergodic capacity of rank-1 Ricean-fading MIMO channels," *IEEE Trans. Inf. Theory*, vol. 53, no. 2, pp. 502–517, Feb. 2007.

[12] F. R. Farrokhi, G. J. Foschini, A. Lozano, and R. A. Valenzuela, "Link-optimal space-time processing with multiple transmit and receive antennas," *IEEE Commun. Lett.*, vol. 5, no. 3, pp. 85–87, Mar. 2001.

[13] S. Wyne, A. F. Molisch, P. Almers, G. Eriksson, J. Karedal, and F. Tufvesson, "Statistical evaluation of outdoor-to-indoor office MIMO measurements at 5.2 GHz," in *Proc. 61st IEEE Veh. Technol. Conf. (VTC)*, Stockholm, Sweden, May 2005, pp. 146–150.

[14] V. Erceg, P. Soma, D. S. Baum, and S. Catreux, "Multiple-input multiple-output fixed wireless radio channel measurements and modeling using dual-polarized antennas at 2.5 GHz," *IEEE Trans. Wireless Commun.*, vol. 3, no. 6, pp. 2288–2298, Nov. 2004.

[15] A. Ispas, J. Hölscher, X. Gong, C. Schneider, G. Ascheid, and R. Thomä, "Modeling and performance evaluation for mobile Ricean MIMO channels," in *Proc. IEEE Int. Conf. Commun. (ICC)*, Ottawa, Canada, Jun. 2012.

[16] M. Landmann, M. Käske, and R. S. Thomä, "Impact of incomplete and inaccurate data models on high resolution parameter estimation in multidimensional channel sounding," *IEEE Trans. Antennas Propag.*, vol. 60, no. 2, pp. 557–573, Feb. 2012.

[17] L. J. Greenstein, D. G. Michelson, and V. Erceg, "Moment-method estimation of the Ricean K-factor," *IEEE Commun. Lett.*, vol. 3, no. 6, pp. 175–176, Jun. 1999.

[18] R. A. Horn and C. R. Johnson, *Matrix Analysis*. Cambridge, UK: Cambridge Univ. Press, 1990.

[19] A. Ispas, C. Schneider, G. Ascheid, and R. Thomä, "Performance evaluation of downlink beamforming over non-stationary channels with interference," in *Proc. 22nd IEEE Int. Symp. Personal, Indoor, Mobile Radio Commun. (PIMRC)*, Toronto, Canada, Sep. 2011, pp. 1677–1681.

[20] N. Jindal and A. Lozano, "Fading models and metrics for contemporary wireless systems," in *Proc. 44th Asilomar Conf. Signals, Syst., Comput.*, Pacific Grove, CA, USA, Nov. 2010, pp. 625–629.

[21] A. Ispas, C. Schneider, G. Ascheid, and R. Thomä, "Analysis of local quasi-stationarity regions in an urban macrocell scenario," in *Proc. 71st IEEE Veh. Technol. Conf. (VTC)*, Taipei, Taiwan, May 2010.

[22] V. Erceg, P. Soma, D. S. Baum, and A. J. Paulraj, "Capacity obtained from multiple-input multiple-output channel measurements in fixed wireless environments at 2.5 GHz," in *Proc. IEEE Int. Conf. Commun. (ICC)*, New York, NY, USA, Apr. 2002, pp. 396–400.

[23] M. Vu and A. Paulraj, "On the capacity of MIMO wireless channels with dynamic CSIT," *IEEE J. Sel. Areas Commun.*, vol. 25, no. 7, pp. 1269–1283, Sep. 2007.

[24] R. A. Horn and C. R. Johnson, *Topics in Matrix Analysis*. Cambridge, UK: Cambridge Univ. Press, 1994.

[25] P. H. M. Janssen and P. Stoica, "On the expectation of the product of four matrix-valued Gaussian random variables," *IEEE Trans. Autom. Control*, vol. 33, no. 9, pp. 867–870, Sep. 1988.